

Chapter 4

Which Diagnostic Modality is best to Assess Benign Hepatic Tumors?

Stephen Thomas and Aytekin Oto

Abstract Benign hepatic lesions are relatively common in the general population. The majority of these lesions are incidentally detected at imaging and don't pose any risk to the patient. Some of these lesions have characteristic imaging features while others can have atypical imaging features and can pose a diagnostic challenge. Utilizing the proper imaging modality and intravenous contrast agents can help better characterize them and minimize unnecessary workup of these lesions.

Benign hepatic lesions are classified according to their cell of origin. This article discusses common and uncommon benign hepatic tumors, their different imaging features, and the diagnostic modality that can best characterize them.

Keywords Hemangioma • Focal nodular hyperplasia • Hepatocellular adenoma • Biliary hamartoma • Medical imaging • Benign liver lesions

Introduction

There is high prevalence of benign hepatic lesions in the general population. While most of these lesions are usually asymptomatic and incidentally detected, they may pose a clinical dilemma in patients with systemic disease, chronic liver disease or in patients with a malignancy undergoing staging. These lesions may require additional imaging to prove benignity or in some cases may need resection due to their size or risk of hemorrhage. The benign hepatic neoplasms include hemangiomas, which are of mesenchymal origin; focal nodular hyperplasia (FNH), hepatocellular adenoma (HCA), and nodular regenerative hyperplasia (NRH) which are of hepatocellular origin; hepatic cysts, bile duct hamartoma which are of cholangiocellular origin.

S. Thomas (✉) • A. Oto
Department of Radiology, The University of Chicago Medicine,
5841 S. Maryland Avenue, MC 2026, Chicago, IL 60637, USA
e-mail: sthomas@hotmail.com

Imaging modalities commonly used for non-invasive liver lesion work-up and characterization includes ultrasonography (US), computed tomography (CT), magnetic resonance (MR) imaging. The tumor features being evaluated include their cystic or solid appearance; calcifications, fat and hemorrhage within the lesion; lesion border and capsule. The use of intravenous contrast agents allows evaluation of lesion vascularity, perfusion, hepatocyte function and biliary excretion.

There is a paucity of prospective studies comparing all modalities and their performance in detection and diagnosis of benign hepatic tumors in the literature. Imaging technologies were introduced at different decades with each modality undergoing significant technological advances over time leading to improved lesion conspicuity and characterization. In many cases, studies comparing the imaging findings of a particular modality with lesion histology have not been performed. Comparison with either another modality or following lesion stability over time would be considered the “gold-standard”. Modalities such as US, CT and MR have improved lesion detection and characterization with the introduction of intravascular contrast agents, including selective hepatobiliary MR contrast agents, which have improved liver lesion characterization. Sonographic contrast agents have provided additional diagnostic capability to conventional ultrasonography. However, although these are widely available in Europe, their availability is limited in the US.

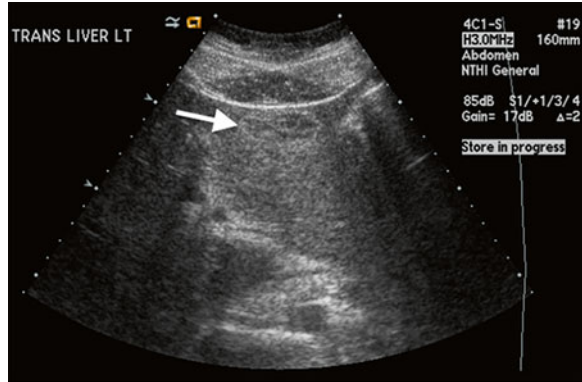
In this chapter, we will discuss the imaging features of cavernous hemangioma, focal nodular hyperplasia, hepatic adenoma, biliary hamartoma, and provide a preferred modality imaging in difficult cases.

Cavernous Hemangioma

Ultrasonography The ‘typical’ imaging features of a small hemangioma (<2 cm) on ultrasound is uniform hyperechogenicity (66 %), well defined margin and posterior acoustic enhancement [1]. Between 20 and 40 % (mostly larger lesions) can have an ‘atypical’ pattern with an echogenic border either as a thick rind or thin rim with a hypoechoic internal echo pattern or an anechoic/cystic pattern (Fig. 4.1) [2, 3]. Hemangiomas detected by ultrasound tend to be stable over time with 82 % having similar imaging characteristics. 18 % can show change in their sonographic appearance and they can also grow in size over the time [4]. The ultrasound appearance of hemangiomas can overlap with those of hepatocellular carcinoma (HCC) and some hypervascular hepatic metastases [5, 6]. As a result, patients with chronic liver disease or with a known or suspected extra-hepatic malignancy should undergo a confirmatory examination such as a contrast enhanced CT or MRI.

Computed Tomography Hemangiomas are well demarcated masses that are hypo-attenuating to liver parenchyma and are iso-attenuating to blood pool on non-contrast CT. Dystrophic calcifications can be present in approximately 10 % of lesions. With contrast administration, hemangiomas have a typical enhancement

Fig. 4.1 Ultrasound of the liver shows a hypoechoic heterogeneous mass within the left lobe of the liver with a hyperechoic rim (arrow)



pattern with peripheral nodular discontinuous enhancement on the arterial and early portal venous phase with gradual centripetal filling on delayed phase images. This enhancement pattern is present in approximately 60 % of all hemangiomas, more commonly present in larger lesions and varies by size: >2 cm (85 %), 1–2 cm (55 %) and <1 cm (23 %) [7]. Smaller lesions can show diffuse hyper-enhancement, a pattern that can be seen in metastasis.

Magnetic Resonance Imaging A typical hemangioma is a well-demarcated homogenous mass that is hypointense on T1-weighted images and hyperintense on T2-weighted images (T2–WI) (Fig. 4.2). The very long T2 relaxation of hemangiomas is useful in distinguishing them from malignant hepatic neoplasms. Hemangiomas demonstrate a relative increase in signal intensity on heavily T2–WI sequences compared to moderately T2–WI sequences. In contradistinction, other solid hepatic masses show a relative decrease in signal intensity on more heavily T2–WI [8–11]. Using a 1.5 Tesla MR unit, MRI can characterize lesions as hemangiomas with an accuracy of 84–97 % based on T2 values, morphologic features and tissue homogeneity [8, 10, 11]. However, hypervascular metastasis from pheochromocytoma, carcinoid, and pancreatic islet-cell tumor can also be hyperintense on T2–WI and is a pitfall of this technique [12, 13]. Therefore, intravenous administered contrast agent is usually required to make a definitive diagnosis of hemangioma. Hemangiomas >4 cm can be heterogeneous in signal due to fibrosis, hemorrhage, thrombosis, hyalinization and cystic degeneration [14, 15].

Use of an intravenous gadolinium based contrast agent (GBCA) results in similar enhancement patterns as CT with arterial peripheral nodular or globular enhancement and progressive centripetal enhancement (Figs. 4.3 and 4.4). This pattern is seen in hemangiomas >2 cm; small lesions <2 cm may have a homogenous enhancement on early phase and may be indistinguishable from small hypervascular metastasis. Metastasis tends to have a continuous rim enhancement on later phases of imaging [12, 13, 16]. Contrast enhanced MRI is able to distinguish hemangioma from metastasis with an accuracy of 96 % [17].

Fig. 4.2 Axial fat saturated T2-weighted MRI shows a well-demarcated T2 hyperintense mass in the left lobe of the liver (*arrow*)

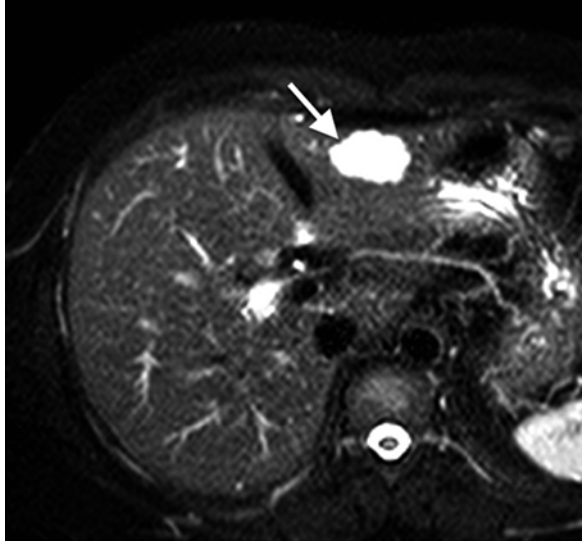
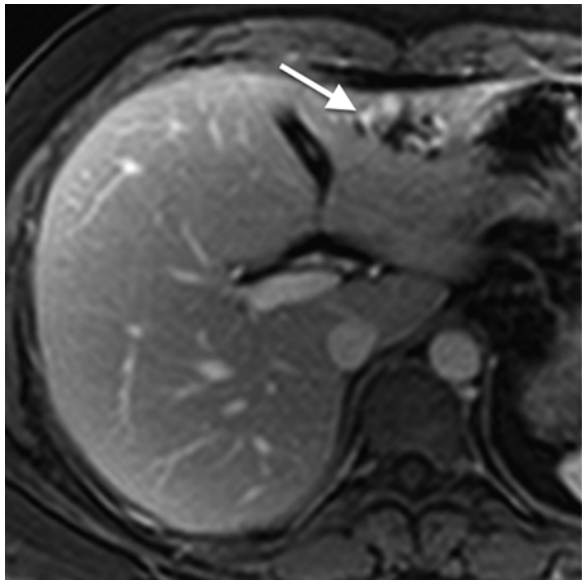


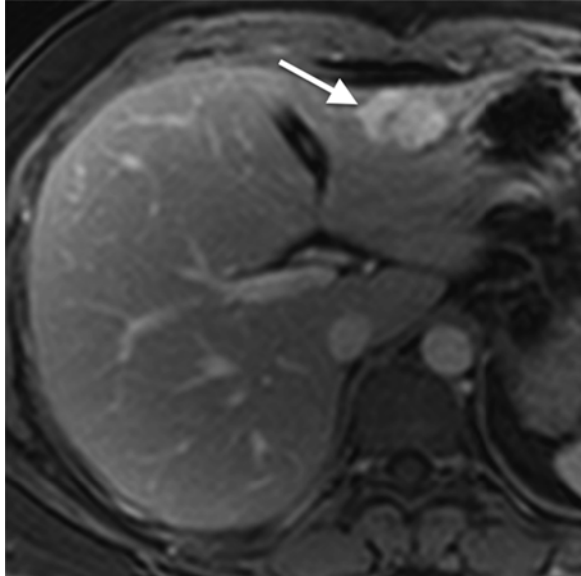
Fig. 4.3 Axial fat saturated T1-FSPGR post contrast MRI shows the classic peripheral nodular discontinuous enhancement on early arterial phase of imaging (*arrow*)



Strategy for Difficult Cases

MRI is the modality of choice in cases where the diagnosis is not certain. The use of heavily weighted T2-WI, multi-phasic contrast sequences with the ability to obtain multiple delayed phases without any ionizing radiation can help confirm the diagnosis of hemangioma. MRI can identify atypical features of hemangiomas,

Fig. 4.4 Axial fat saturated T1-FSPGR post contrast MRI shows the progressive centripetal enhancement on portal phase of imaging with the mass filling in and remaining iso-intense to vasculature (*arrow*)



which include incomplete contrast filling, seen in hemangiomas larger than 3 cm due to central scarring. Lesions greater than 5 cm can have “flame shaped” discontinuous peripheral enhancement which may dominate or coexist with the typical nodular enhancement [18]. Hyalinized hemangiomas can be predominately fibrosed with obliterated vascular spaces and may not enhance. They may be only be slightly hyperintense on T2-WI, lack the early enhancement on dynamic contrast enhancement, with slight peripheral enhancement on late phase and may be confidently diagnosed on MR [19].

Focal Nodular Hyperplasia

Ultrasonography FNH are frequently first identified on US as the modality is commonly used to evaluate the liver and gallbladder. However, FNH echotexture can be quite variable. They can appear hyper, hypo, and isoechoic relative to hepatic parenchyma. Isoechoic lesions may only be detected if they deform the hepatic contour. Frequently, FNH are located in the subcapsular area of the liver and may deform the liver contour or rarely may be exophytic. The central scar, which is an important imaging feature, is only present in about 20 % of cases. Gray scale sonography is unable to reliably distinguish FNH from other neoplastic lesions [20].

Computed Tomography Detection and characterization of FNH is done using a tri-phasic contrast enhanced CT. On unenhanced CT, FNH is usually a homogenous isoattenuating or hypoattenuating mass. On arterial phase, FNH has marked arterial

Fig. 4.5 Contrast enhanced CT shows a right hepatic lobe mass that is nearly iso-attenuating to the hepatic parenchyma (*arrow*). The lesion has a small hypo-attenuating central scar (*arrow head*)



enhancement that is homogeneous [20–22]. In about 30 % of cases a visible central scar is present which does not enhance on early phases of imaging and can be very small [20, 23]. In larger lesions, feeding hepatic arteries, small central and septal arteries, and early draining veins can be present [22, 24]. On portal venous and delayed phases, FNHs are iso-attenuating to hepatic parenchyma (Fig. 4.5). Enhancement of the central scar can be seen on delayed phases of imaging when it contains myxomatous stroma [23, 25]. While no prospective studies exist regarding the accuracy of CT to detect and characterize FNH, a small retrospective series (n=20) showed that CT had a sensitivity of 70 % and specificity of 92 % and led to the correct characterization in 78 % of cases [26]. In a larger series of 86 patients with 99 foci of FNH, CT was able to correctly diagnose FNH in 60.3 % of cases [27].

Magnetic Resonance Imaging On unenhanced MR, FNH has similar characteristics to hepatic parenchyma on T1- and T2-weighted sequences [28]. Atypical features include hyperintense appearance on T1-WI due to steatosis, sinusoidal dilatation, or hemorrhage [28]. The central scar can be present in 25–43 % of lesions and is T1 hypointense and T2 hyperintense (Fig. 4.6) due to presence of vascular channels and bile ductules [29–32].

Using IV GBCA, typically FNH has homogenous arterial enhancement and is isointense to liver on portal venous phase. The central scar can be present in 79 % of FNH and is hyperintense due to enhancement on delayed phase of imaging (Figs. 4.7 and 4.8) [32].

Hepatobiliary contrast agents are unique MR contrast agents in that they are taken up by functioning hepatocytes and excreted with bile. Hepatobiliary GBCAs such as

Fig. 4.6 Axial fat suppressed T2 weighted MRI shows a mildly hyperintense mass (*arrow*) with a hyperintense central scar (*arrow head*)

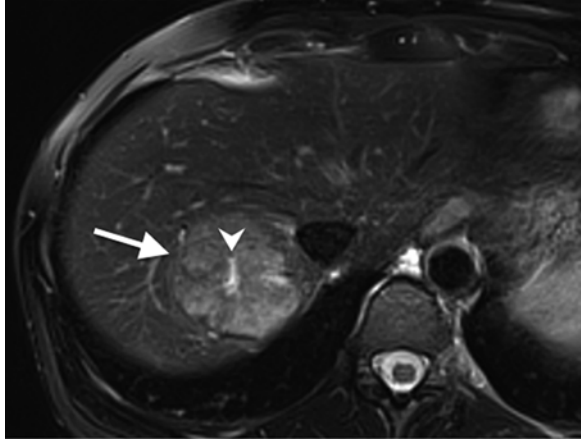
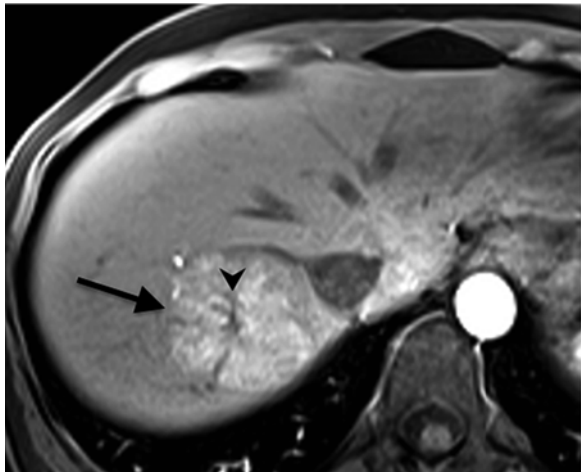


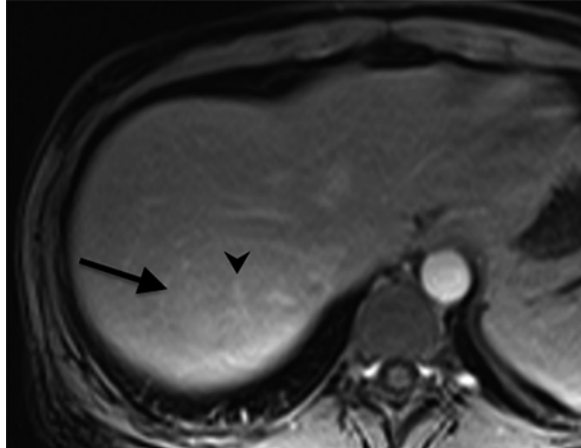
Fig. 4.7 Axial fat saturated T1-FSPGR post contrast MRI shows hyper-enhancement of the mass on arterial phase (*black arrow*). The central scar does not enhance (*arrow head*)



Gd-BOPTA and Gd-EOB-DTPA have properties of an extracellular contrast agent providing dynamic contrast enhancement information and biliary excretion for delayed hepatobiliary imaging performed 20 min after contrast bolus injection. Lesions that contain functioning hepatocytes show contrast uptake. Since FNH contain functioning hepatocytes, on delayed phase of imaging, they are typically hyperintense to isointense to hepatic parenchyma [31, 33].

The sensitivity and specificity of MRI in differentiating FHN from hepatocellular adenoma (HCA) is 96.9 %, and 100 %, and is primarily based on the contrast washout on hepatobiliary phase in hepatic adenomas when using Gd-BOPTA in a prospective study [34]. Using Gd-EOB-DTPA and the hepatobiliary phase the sensitivity to detect FNH was 96 % with a positive predictive value of 96 % when compared to HCA [35].

Fig. 4.8 Axial fat saturated T1-FSPGR post contrast MRI shows the mass to be iso-attenuating to the liver on portal venous phase (*black arrow*). The central scar now enhances, characteristic of focal nodular hyperplasia (*arrow head*)



Strategy for Difficult Cases

MRI using a hepatobiliary specific contrast agent may characterize lesions that cannot be otherwise characterized by CT. Atypical FNH lesions may show only mild arterial enhancement, and may be hypointense to liver parenchyma on late dynamic phase. For these lesions adding a hepatobiliary phase and calculating a signal intensity (SI) ratio improves diagnostic yield. Using a cutoff value of 0.87 for the SI ratio during the hepatobiliary phase, the sensitivity and specificity for differentiating FNH from HCA was 92 % and 91 % respectively [36].

Hepatocellular Adenoma

Ultrasonography HCA have a heterogeneous variable echotexture with 80 % having a mixed echogenicity and 20 % purely hypoechoic [37]. In a small study of 27 cases of HCA, the lesions were hypoechoic to hepatic parenchyma in 41 %, 30 % are hyperechoic, 22 % are isoechoic, and 7 % are of mixed echogenicity [21]. The utility of gray scale ultrasound to characterize HCA is limited due the overlap of imaging features with other benign and malignant hepatic lesions.

Computed Tomography HCAs have a variable appearance on unenhanced CT images. They may be hypoattenuating due to the presence of intracellular lipid, old hemorrhage or necrosis, or it may be hyperattenuating from acute hemorrhage or large amounts of glycogen [37]. HCA are sharply marginated – 85 %, nonlobulated – 95 %, sometimes encapsulated – 30 %, and rarely can calcify 5–10 %. Necrosis or hemorrhage can occur in 25 % of lesions [38, 39]. HCAs are almost uniformly (80–100 %) hyperattenuating on hepatic arterial phase and have variable appearance on portal venous phase with 31 % remaining hyperattenuating, 44 %

isoattenuating, and 25 % hypoattenuating [39, 40]. On delayed phase CT, HCAs characteristically are hypoattenuating to liver parenchyma with few (6 %) that are hyperattenuating [39]. The enhancement pattern helps differentiate FNH from HCA, which is important for patient management. HCA however have similar contrast enhancement characteristics as hepatocellular carcinoma (HCC) and differentiation between the lesions can be problematic especially in lesions that have undergone hemorrhage [41].

Magnetic Resonance Imaging HCAs have a variable appearance on MRI as there are sub-types including inflammatory, steatotic or those with β -catenin activation.

The inflammatory subtype accounts for 30–50 % of adenomas. These lesions are mildly hyperintense on T2–WI especially in the periphery of the lesion (Fig. 4.9), and iso to hypointense on T1–WI with heterogeneous signal intensity. There is characteristic T2 hyperintense rim like band termed the atoll sign in the periphery of the lesion that is iso-intense to surrounding liver toward the center of the lesion can be seen in 43 % of inflammatory HCAs [42].

Inflammatory HCAs are diffusely hyperintense on arterial enhancement persisting into the portal venous and delayed phases (Figs. 4.10 and 4.11). The T2 hyperintensity and persistent enhancement together are 85.2 % sensitive and 87.5 % specific for the diagnosis [43].

The steatotic subtype, shows diffuse signal loss on chemical shift sequence due to homogenous intratumoral fat. These lesions show moderate arterial enhancement not persisting into the portal venous phase [43]. The presence of intratumoral fat is not specific for HCAs as up to 40 % of hepatocellular carcinomas may contain fat [44].

Fig. 4.9 Axial fat suppressed T2 weighted MRI shows a mildly hyperintense mass (*arrow*) in the right lobe of the liver and larger mass in the left lobe of the liver (*arrow head*)



Fig. 4.10 Axial fat saturated T1-FSPGR post contrast MRI shows brisk homogenous enhancement of the right hepatic lobe mass (*arrow*) and the larger left hepatic lobe mass (*arrow head*) during arterial phase of imaging



Fig. 4.11 Axial fat saturated T1-FSPGR post contrast MRI shows the right hepatic lobe mass (*arrow*) and the left hepatic lobe mass (*arrow head*) remain hyperintense to liver on portal venous phase



HCA with β -catenin activation can have non-specific imaging features with strong arterial enhancement and portal venous washout. MRI may not be able to definitively characterize these lesions as the imaging features can overlap with HCC [43]. HCAs with activated β -catenin present a high risk of malignant transformation [45].

Fig. 4.12 Axial fat saturated T1-FSPGR post contrast MRI performed with a hepatobiliary contrast agent and imaged during the hepatobiliary phase (20 min after injection) shows no retention of contrast in the right hepatic lobe mass compatible with a hepatic adenoma (*arrow*). The left hepatic lobe mass retains contrast and is compatible with focal nodular hyperplasia (*arrow head*)



Strategy for Difficult Cases

Since HCAs can have several subtypes, undergo hemorrhage, and have variable imaging features on conventional MRI, they may not be easily discriminated from FNHs. Using hepatobiliary contrast agents on MR will improve the diagnostic performance of MRI. Delayed hepatobiliary phase images can be used to separate HCA from FNH with the former appearing hypointense to liver (Fig. 4.12) [34]. Follow-up studies have shown that up to 71 % of inflammatory HCAs can have areas of iso- or hyperintensity to the surrounding liver in the hepatocyte phase [46].

Biliary Hamartoma

Ultrasonography Biliary hamartomas have a variable appearance on ultrasound. They usually present as tiny hypoechoic or hyperechoic foci measuring less than 10 mm scattered through out the liver and may be associated with comet-tail artifacts (Fig. 4.13) [47, 48]. Their variable appearance on sonography may be mistaken for metastasis.

Computed Tomography At unenhanced CT, biliary hamartomas appear as well-marginated hypo or iso-attenuating lesions of nearly uniform size that do not enhance on contrast administration (Fig. 4.14) [48]. Their imaging features are important to recognize as they may simulate metastases or microabscesses [49, 50].

Fig. 4.13 Ultrasound of the liver shows increased parenchymal echogenicity of the right lobe with multiple small echogenic interfaces



Fig. 4.14 Contrast enhanced CT shows multiple small nearly uniformly hypo-attenuating lesions in the liver (*arrow heads*). No clear enhancing wall is seen



Magnetic Resonance Imaging Biliary hamartomas have a characteristic appearance at MRI. They are hypointense on T1–WI, well defined and hyper-intense on T2–WI (Fig. 4.15). With GBCA they do not have central enhancement but may have a thin rim of peripheral enhancement, which may be from compressed hepatic parenchyma (Fig. 4.16) [51].

Fig. 4.15 Axial T2 weighted MRI shows multiple small nearly uniformly sized T2 hyperintense lesions (*arrow heads*)

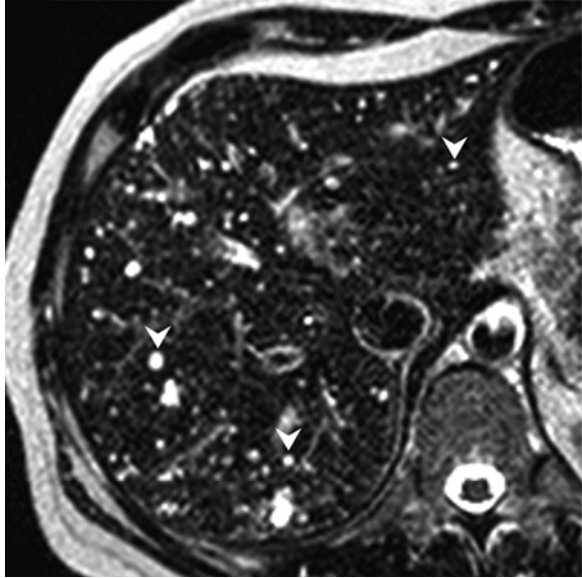
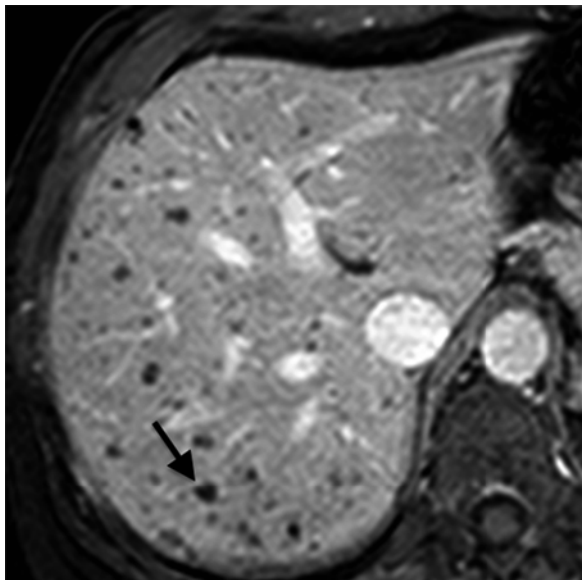


Fig. 4.16 Axial fat saturated T1-FSPGR post contrast MRI shows multiple small nearly uniformly sized hypointense lesions in the liver. Some have a subtle perceivable wall (*arrow*), which represents compressed hepatic parenchyma



Conclusion

Focal liver lesions are commonly encountered during routine imaging. While US and CT are able to detect and characterize many lesions, MR imaging with hepatocyte specific contrast agents can be used for difficult lesions and may be able to

definitively characterize liver lesions so as to avoid biopsy or surgery. However, for lesions that do not have typical imaging features or those that are complicated by hemorrhage may have to undergo biopsy for accurate diagnosis.

References

1. Mirk P, Rubaltelli L, Bazzocchi M, et al. Ultrasonographic patterns in hepatic hemangiomas. *J Clin Ultrasound*. 1982;10:373–8.
2. Moody AR, Wilson SR. Atypical hepatic hemangioma: a suggestive sonographic morphology. *Radiology*. 1993;188:413–7.
3. Ricci OE, Fanfani S, Calabro A, et al. Diagnostic approach to hepatic hemangiomas detected by ultrasound. *Hepatogastroenterology*. 1985;32:53–6.
4. Gibney RG, Hendin AP, Cooperberg PL. Sonographically detected hepatic hemangiomas: absence of change over time. *AJR Am J Roentgenol*. 1987;149:953–7.
5. Leifer DM, Middleton WD, Teefey SA, Menias CO, Leahy JR. Follow-up of patients at low risk for hepatic malignancy with a characteristic hemangioma at US. *Radiology*. 2000;214:167–72.
6. Rapaccini GL, Pompili M, Caturelli E, et al. Hepatocellular carcinomas <2 cm in diameter complicating cirrhosis: ultrasound and clinical features in 153 consecutive patients. *Liver Int*. 2004;24:124–30.
7. Yun EJ, Choi BI, Han JK, et al. Hepatic hemangioma: contrast-enhancement pattern during the arterial and portal venous phases of spiral CT. *Abdom Imaging*. 1999;24:262–6.
8. McFarland EG, Mayo-Smith WW, Saini S, Hahn PF, Goldberg MA, Lee MJ. Hepatic hemangiomas and malignant tumors: improved differentiation with heavily T2-weighted conventional spin-echo MR imaging. *Radiology*. 1994;193:43–7.
9. Ohtomo K, Itai Y, Furui S, Yashiro N, Yoshikawa K, Iio M. Hepatic tumors: differentiation by transverse relaxation time (T2) of magnetic resonance imaging. *Radiology*. 1985;155:421–3.
10. Ohtomo K, Itai Y, Yoshikawa K, Kokubo T, Iio M. Hepatocellular carcinoma and cavernous hemangioma: differentiation with MR imaging. Efficacy of T2 values at 0.35 and 1.5 T. *Radiology*. 1988;168:621–3.
11. Stark DD, Felder RC, Wittenberg J, et al. Magnetic resonance imaging of cavernous hemangioma of the liver: tissue-specific characterization. *AJR Am J Roentgenol*. 1985;145:213–22.
12. Berger JF, Laissy JP, Limot O, et al. Differentiation between multiple liver hemangiomas and liver metastases of gastrinomas: value of enhanced MRI. *J Comput Assist Tomogr*. 1996;20:349–55.
13. Soyer P, Gueye C, Somveille E, Laissy JP, Scherrer A. MR diagnosis of hepatic metastases from neuroendocrine tumors versus hemangiomas: relative merits of dynamic gadolinium chelate-enhanced gradient-recalled echo and unenhanced spin-echo images. *AJR Am J Roentgenol*. 1995;165:1407–13.
14. Choi BI, Han MC, Park JH, Kim SH, Han MH, Kim CW. Giant cavernous hemangioma of the liver: CT and MR imaging in 10 cases. *AJR Am J Roentgenol*. 1989;152:1221–6.
15. Ros PR, Lubbers PR, Olmsted WW, Morillo G. Hemangioma of the liver: heterogeneous appearance on T2-weighted images. *AJR Am J Roentgenol*. 1987;149:1167–70.
16. Whitney WS, Herfkens RJ, Jeffrey RB, et al. Dynamic breath-hold multiplanar spoiled gradient-recalled MR imaging with gadolinium enhancement for differentiating hepatic hemangiomas from malignancies at 1.5 T. *Radiology*. 1993;189:863–70.
17. Mitchell DG, Saini S, Weinreb J, et al. Hepatic metastases and cavernous hemangiomas: distinction with standard- and triple-dose gadoteridol-enhanced MR imaging. *Radiology*. 1994;193:49–57.

18. Danet IM, Semelka RC, Braga L, Armao D, Woosley JT. Giant hemangioma of the liver: MR imaging characteristics in 24 patients. *Magn Reson Imaging*. 2003;21:95–101.
19. Cheng HC, Tsai SH, Chiang JH, Chang CY. Hyalinized liver hemangioma mimicking malignant tumor at MR imaging. *AJR Am J Roentgenol*. 1995;165:1016–7.
20. Shamsi K, De Schepper A, Degryse H, Deckers F. Focal nodular hyperplasia of the liver: radiologic findings. *Abdom Imaging*. 1993;18:32–8.
21. Mathieu D, Bruneton JN, Drouillard J, Pointreau CC, Vasile N. Hepatic adenomas and focal nodular hyperplasia: dynamic CT study. *Radiology*. 1986;160:53–8.
22. Choi CS, Freeny PC. Triphasic helical CT of hepatic focal nodular hyperplasia: incidence of atypical findings. *AJR Am J Roentgenol*. 1998;170:391–5.
23. Carlson SK, Johnson CD, Bender CE, Welch TJ. CT of focal nodular hyperplasia of the liver. *AJR Am J Roentgenol*. 2000;174:705–12.
24. Brancatelli G, Federle MP, Katyal S, Kapoor V. Hemodynamic characterization of focal nodular hyperplasia using three-dimensional volume-rendered multidetector CT angiography. *AJR Am J Roentgenol*. 2002;179:81–5.
25. Mortelet KJ, Praet M, Van Vlierberghe H, Kunnen M, Ros PR. CT and MR imaging findings in focal nodular hyperplasia of the liver: radiologic-pathologic correlation. *AJR Am J Roentgenol*. 2000;175:687–92.
26. Procacci C, Fugazzola C, Cinquino M, et al. Contribution of CT to characterization of focal nodular hyperplasia of the liver. *Gastrointest Radiol*. 1992;17:63–73.
27. Shen YH, Fan J, Wu ZQ, et al. Focal nodular hyperplasia of the liver in 86 patients. *Hepatobiliary Pancreat Dis Int*. 2007;6:52–7.
28. Ferlicot S, Kobeiter H, Tran Van Nhieu J, et al. MRI of atypical focal nodular hyperplasia of the liver: radiology-pathology correlation. *AJR Am J Roentgenol*. 2004;182:1227–31.
29. Vilgrain V, Flejou JF, Arrive L, et al. Focal nodular hyperplasia of the liver: MR imaging and pathologic correlation in 37 patients. *Radiology*. 1992;184:699–703.
30. Rummeny E, Weissleder R, Sironi S, et al. Central scars in primary liver tumors: MR features, specificity, and pathologic correlation. *Radiology*. 1989;171:323–6.
31. Grazioli L, Morana G, Federle MP, et al. Focal nodular hyperplasia: morphologic and functional information from MR imaging with gadobenate dimeglumine. *Radiology*. 2001;221:731–9.
32. Mahfouz AE, Hamm B, Taupitz M, Wolf KJ. Hypervascular liver lesions: differentiation of focal nodular hyperplasia from malignant tumors with dynamic gadolinium-enhanced MR imaging. *Radiology*. 1993;186:133–8.
33. Huppertz A, Haraida S, Kraus A, et al. Enhancement of focal liver lesions at gadoxetic acid-enhanced MR imaging: correlation with histopathologic findings and spiral CT – initial observations. *Radiology*. 2005;234:468–78.
34. Grazioli L, Morana G, Kirchin MA, Schneider G. Accurate differentiation of focal nodular hyperplasia from hepatic adenoma at gadobenate dimeglumine-enhanced MR imaging: prospective study. *Radiology*. 2005;236:166–77.
35. Bieze M, van den Esschert JW, Nio CY, et al. Diagnostic accuracy of MRI in differentiating hepatocellular adenoma from focal nodular hyperplasia: prospective study of the additional value of gadoxetate disodium. *AJR Am J Roentgenol*. 2012;199:26–34.
36. Grazioli L, Bondioni MP, Haradome H, et al. Hepatocellular adenoma and focal nodular hyperplasia: value of gadoxetic acid-enhanced MR imaging in differential diagnosis. *Radiology*. 2012;262:520–9.
37. Welch TJ, Sheedy 2nd PF, Johnson CM, et al. Focal nodular hyperplasia and hepatic adenoma: comparison of angiography, CT, US, and scintigraphy. *Radiology*. 1985;156:593–5.
38. Grazioli L, Federle MP, Ichikawa T, Balzano E, Nalesnik M, Madariaga J. Liver adenomatosis: clinical, histopathologic, and imaging findings in 15 patients. *Radiology*. 2000;216:395–402.
39. Ichikawa T, Federle MP, Grazioli L, Nalesnik M. Hepatocellular adenoma: multiphasic CT and histopathologic findings in 25 patients. *Radiology*. 2000;214:861–8.

40. Grazioli L, Federle MP, Brancatelli G, Ichikawa T, Olivetti L, Blachar A. Hepatic adenomas: imaging and pathologic findings. *Radiographics*. 2001;21:877–92; discussion 892–874.
41. Hussain SM, van den Bos IC, Dwarkasing RS, Kuiper JW, den Hollander J. Hepatocellular adenoma: findings at state-of-the-art magnetic resonance imaging, ultrasound, computed tomography and pathologic analysis. *Eur Radiol*. 2006;16:1873–86.
42. van Aalten SM, Thomeer MG, Terkivatan T, et al. Hepatocellular adenomas: correlation of MR imaging findings with pathologic subtype classification. *Radiology*. 2011;261:172–81.
43. Laumonier H, Bioulac-Sage P, Laurent C, Zucman-Rossi J, Balabaud C, Trillaud H. Hepatocellular adenomas: magnetic resonance imaging features as a function of molecular pathological classification. *Hepatology*. 2008;48:808–18.
44. Paulson EK, McClellan JS, Washington K, Spritzer CE, Meyers WC, Baker ME. Hepatic adenoma: MR characteristics and correlation with pathologic findings. *AJR Am J Roentgenol*. 1994;163:113–6.
45. Bioulac-Sage P, Rebouissou S, Thomas C, et al. Hepatocellular adenoma subtype classification using molecular markers and immunohistochemistry. *Hepatology*. 2007;46:740–8.
46. Thomeer MG, Willemsen FE, Biermann KK, et al. MRI features of inflammatory hepatocellular adenomas on hepatocyte phase imaging with liver-specific contrast agents. *J Magn Reson Imaging*. 2014;39:1259–64.
47. Zheng RQ, Zhang B, Kudo M, Onda H, Inoue T. Imaging findings of biliary hamartomas. *World J Gastroenterol*. 2005;11:6354–9.
48. Lev-Toaff AS, Bach AM, Wechsler RJ, Hilpert PL, Gatalica Z, Rubin R. The radiologic and pathologic spectrum of biliary hamartomas. *AJR Am J Roentgenol*. 1995;165:309–13.
49. Sada PN, Ramakrishna B. Computed tomography of von Meyenburg complex simulating micro-abscesses. *Australas Radiol*. 1994;38:225–6.
50. Eisenberg D, Hurwitz L, Yu AC. CT and sonography of multiple bile-duct hamartomas simulating malignant liver disease (case report). *AJR Am J Roentgenol*. 1986;147:279–80.
51. Semelka RC, Hussain SM, Marcos HB, Woosley JT. Biliary hamartomas: solitary and multiple lesions shown on current MR techniques including gadolinium enhancement. *J Magn Reson Imaging*. 1999;10:196–201.